BRAIN
A JOURNAL OF NEUROLOGY

Structural brain abnormalities in the common epilepsies assessed in a worldwide ENIGMA study

Christopher D. Whelan,[1,2] Andre Altmann,[3] Juan A. Botía,[4] Neda Jahanshad,[1]
Derrek P. Hibar,[1] Julie Absil,[5] Saud Alhusaini,[2,6] Marina K. M. Alvim,[7] Pia Auvinen,[8,9]
Emanuele Bartolini,[10,11] Felipe P. G. Bergo,[7] Tauana Bernardes,[7] Karen Blackmon,[12,13]
Barbara Braga,[7] Maria Eugenia Caligiuri,[14] Anna Calvo,[15] Sarah J. Carr,[16] Jian Chen,[17]
Shuai Chen,[18,19] Andrea Cherubini,[14] Philippe David,[5] Martin Domin,[20] Sonya Foley,[21]
Wendy França,[7] Gerrit Haaker,[22,23] Dmitry Isaev,[1] Simon S. Keller,[24]
Raviteja Kotikalapudi,[25,26] Magdalena A. Kowalczyk,[27] Ruben Kuzniecky,[12]
Soenke Langner,[20] Matteo Lenge,[10] Kelly M. Leyden,[28,29] Min Liu,[30] Richard Q. Loi,[28,29]
Pascal Martin,[25] Mario Mascalchi,[31,32] Marcia E. Morita,[7] Jose C. Pariente,[15] Raul Rodríguez-Cruces,[33] Christian Rummel,[34] Taavi Saavalainen,[9,35] Mira K. Semmelroch,[27]
Mariasavina Severino,[36] Rhys H. Thomas,[37,38] Manuela Tondelli,[39] Domenico Tortora,[36]
Anna Elisabetta Vaudano,[39] Lucy Vivash,[40,41] Felix von Podewils,[42] Jan Wagner,[43,44]
Bernd Weber,[43,45] Yi Yao,[46] Clarissa L. Yasuda,[7] Guohao Zhang,[47] UK Brain Expression
Consortium, Nuria Bargalló,[15,48] Benjamin Bender,[26] Neda Bernasconi,[30]
Andrea Bernasconi,[30] Boris C. Bernhardt,[30,49] Ingmar Blümcke,[23] Chad Carlson,[12,50]
Gianpiero L. Cavalleri,[2,51] Fernando Cendes,[7] Luis Concha,[33] Norman Delanty,[2,51,52]
Chantal Depondt,[53] Orrin Devinsky,[12] Colin P. Doherty,[51,54] Niels K. Focke,[25,55]
Antonio Gambardella,[14,56] Renzo Guerrini,[10,11] Khalid Hamandi,[37,38]
Graeme D. Jackson,[27,57] Reetta Kälviäinen,[8,9] Peter Kochunov,[58] Patrick Kwan,[41]
Angelo Labate,[14,56] Carrie R. McDonald,[28,29] Stefano Meletti,[39] Terence J. O'Brien,[41,59]
Sebastien Ourselin,[3] Mark P. Richardson,[16,60] Pasquale Striano,[61] Thomas Thesen,[12,13]
Roland Wiest,[34] Junsong Zhang,[18,19] Annamaria Vezzani,[62] Mina Ryten,[4,63]
Paul M. Thompson[1] and Sanjay M. Sisodiya[64,65] for the ENIGMA-Epilepsy Working Group

Progressive functional decline in the epilepsies is largely unexplained. We formed the ENIGMA-Epilepsy consortium to understand factors that influence brain measures in epilepsy, pooling data from 24 research centres in 14 countries across Europe, North and South America, Asia, and Australia. Structural brain measures were extracted from MRI brain scans across 2149 individuals with epilepsy, divided into four epilepsy subgroups including idiopathic generalized epilepsies ($n = 367$), mesial temporal lobe epilepsies with hippocampal sclerosis (MTLE; left, $n = 415$; right, $n = 339$), and all other epilepsies in aggregate ($n = 1026$), and compared to 1727 matched healthy controls. We ranked brain structures in order of greatest differences between patients and controls, by meta-analysing effect sizes across 16 subcortical and 68 cortical brain regions. We also tested effects of duration of disease, age at onset, and age-by-diagnosis interactions on structural measures. We observed widespread patterns of altered subcortical volume and reduced cortical grey matter thickness. Compared to controls, all epilepsy groups showed lower volume in the right thalamus

(Cohen's $d = -0.24$ to -0.73; $P < 1.49 \times 10^{-4}$), and lower thickness in the precentral gyri bilaterally ($d = -0.34$ to -0.52; $P < 4.31 \times 10^{-6}$). Both MTLE subgroups showed profound volume reduction in the ipsilateral hippocampus ($d = -1.73$ to -1.91, $P < 1.4 \times 10^{-19}$), and lower thickness in extrahippocampal cortical regions, including the precentral and paracentral gyri, compared to controls ($d = -0.36$ to -0.52; $P < 1.49 \times 10^{-4}$). Thickness differences of the ipsilateral temporopolar, parahippocampal, entorhinal, and fusiform gyri, contralateral pars triangularis, and bilateral precuneus, superior frontal and caudal middle frontal gyri were observed in left, but not right, MTLE ($d = -0.29$ to -0.54; $P < 1.49 \times 10^{-4}$). Contrastingly, thickness differences of the ipsilateral pars opercularis, and contralateral transverse temporal gyrus, were observed in right, but not left, MTLE ($d = -0.27$ to -0.51; $P < 1.49 \times 10^{-4}$). Lower subcortical volume and cortical thickness associated with a longer duration of epilepsy in the all-epilepsies, all-other-epilepsies, and right MTLE groups (beta, $b < -0.0018$; $P < 1.49 \times 10^{-4}$). In the largest neuroimaging study of epilepsy to date, we provide information on the common epilepsies that could not be realistically acquired in any other way. Our study provides a robust ranking of brain measures that can be further targeted for study in genetic and neuropathological studies. This worldwide initiative identifies patterns of shared grey matter reduction across epilepsy syndromes, and distinctive abnormalities between epilepsy syndromes, which inform our understanding of epilepsy as a network disorder, and indicate that certain epilepsy syndromes involve more widespread structural compromise than previously assumed.

1 Imaging Genetics Center, Mark and Mary Stevens Neuroimaging and Informatics Institute, University of Southern California, Los Angeles, California, USA
2 Department of Molecular and Cellular Therapeutics, Royal College of Surgeons in Ireland, Dublin, Ireland
3 Translational Imaging Group, Centre for Medical Image Computing, University College London, London, UK
4 Reta Lila Weston Institute and Department of Molecular Neuroscience, UCL Institute of Neurology, London WC1N 3BG, UK
5 Department of Radiology, Hôpital Erasme, Universite Libre de Bruxelles, Brussels 1070, Belgium
6 Department of Neurology and Neurosurgery, Montreal Neurological Institute, McGill University, Montreal, Quebec, Canada
7 Department of Neurology, University of Campinas, Campinas, Brazil
8 Epilepsy Center, Department of Neurology, Kuopio University, Kuopio, Finland
9 Institute of Clinical Medicine, Neurology, University of Eastern Finland, Kuopio, Finland
10 Pediatric Neurology Unit, Children's Hospital A. Meyer-University of Florence, Italy
11 IRCCS Stella Maris Foundation, Pisa, Italy
12 Comprehensive Epilepsy Center, Department of Neurology, New York University School of Medicine, New York, USA
13 Department of Physiology, Neuroscience and Behavioral Science, St. George's University, Grenada, West Indies
14 Institute of Molecular Bioimaging and Physiology of the National Research Council (IBFM-CNR), Catanzaro, Italy
15 Magnetic Resonance Image Core Facility, IDIBAPS, Barcelona, Spain
16 Department of Basic and Clinical Neuroscience, Institute of Psychiatry, Psychology and Neuroscience, King's College London, UK
17 Department of Computer Science and Engineering, The Ohio State University, USA
18 Cognitive Science Department, Xiamen University, Xiamen, China
19 Fujian Key Laboratory of the Brain-like Intelligent Systems, China
20 Functional Imaging Unit, Institute of Diagnostic Radiology and Neuroradiology, University Medicine Greifswald, Greifswald, Germany
21 Cardiff University Brain Research Imaging Centre, School of Psychology, Wales, UK
22 Department of Neurosurgery, University Hospital, Freiburg, Germany
23 Department of Neuropathology, University Hospital Erlangen, Germany
24 Department of Molecular and Clinical Pharmacology, Institute of Translational Medicine, University of Liverpool, UK
25 Department of Neurology and Epileptology, Hertie Institute for Clinical Brain Research, University of Tübingen, Tübingen, Germany
26 Department of Diagnostic and Interventional Neuroradiology, University of Tübingen, Tübingen, Germany
27 The Florey Institute of Neuroscience and Mental Health, Austin Campus, Melbourne, VIC, Australia
28 Multimodal Imaging Laboratory, University of California San Diego, San Diego, California, USA
29 Department of Psychiatry, University of California San Diego, San Diego, California, USA
30 Neuroimaging of Epilepsy Laboratory, Montreal Neurological Institute and Hospital, Mcgill University, Montreal, Quebec, Canada
31 Neuroradiology Unit, Children's Hospital A. Meyer, Florence, Italy
32 "Mario Serio" Department of Experimental and Clinical Biomedical Sciences, University of Florence, Italy
33 Instituto de Neurobiología, Universidad Nacional Autónoma de México. Querétaro, Querétaro, México
34 Support Center for Advanced Neuroimaging (SCAN), University Institute for Diagnostic and Interventional Neuroradiology, Inselspital, University of Bern, Bern, Switzerland
35 Central Finland Central Hospital, Medical Imaging Unit, Jyväskylä, Finland
36 Neuroradiology Unit, Department of Head and Neck and Neurosciences, Istituto Giannina Gaslini, Genova, Italy
37 Institute of Psychological Medicine and Clinical Neurosciences, Hadyn Ellis Building, Maindy Road, Cardiff, UK
38 Department of Neurology, University Hospital of Wales, Cardiff, UK

39 Department of Biomedical, Metabolic, and Neural Science, University of Modena and Reggio Emilia, NOCSE Hospital, Modena, Italy
40 Melbourne Brain Centre, Department of Medicine, University of Melbourne, Parkville, VIC, 3052, Australia
41 Department of Neurology, Royal Melbourne Hospital, Parkville, 3050, Australia
42 Department of Neurology, University Medicine Greifswald, Greifswald, Germany
43 Department of Epileptology, University Hospital Bonn, Bonn, Germany
44 Department of Neurology, Philips University of Marburg, Marburg Germany
45 Department of Neurocognition / Imaging, Life&Brain Research Centre, Bonn, Germany
46 The Affiliated Chenggong Hospital of Xiamen University, Xiamen, China
47 Department of Computer Science and Electrical Engineering, University of Maryland, Baltimore County, USA
48 Centre de Diagnostic Per la Imatge (CDIC), Hospital Clinic, Barcelona, Spain
49 Multimodal Imaging and Connectome Analysis Lab, Montreal Neurological Institute and Hospital, McGill University, Montreal, Quebec, Canada
50 Medical College of Wisconsin, Department of Neurology, Milwaukee, WI, USA
51 FutureNeuro Research Centre, RCSI, Dublin, Ireland
52 Division of Neurology, Beaumont Hospital, Dublin 9, Ireland
53 Department of Neurology, Hôpital Erasme, Universite Libre de Bruxelles, Brussels 1070, Belgium
54 Neurology Department, St. James's Hospital, Dublin 8, Ireland
55 Department of Clinical Neurophysiology, University Medicine Göttingen, Göttingen, Germany
56 Institute of Neurology, University "Magna Græcia", Catanzaro, Italy
57 Florey Department of Neuroscience and Mental Health, The University of Melbourne, Melbourne, VIC, Australia
58 Maryland Psychiatric Research Center, Department of Psychiatry, University of Maryland School of Medicine, Maryland, USA
59 Department of Medicine, University of Melbourne, Parkville, VIC, 3052, Australia
60 Department of Neurology, King's College Hospital, London, UK
61 Pediatric Neurology and Muscular Diseases Unit, Department of Neurosciences, Rehabilitation, Ophthalmology, Genetics, Maternal and Child Health, University of Genoa, Genova, Italy
62 Dept of Neuroscience, Mario Negri Institute for Pharmacological Research, Via G. La Masa 19, 20156 Milano, Italy
63 Department of Medical and Molecular Genetics, King's College London, London SE1 9RT, UK
64 Department of Clinical and Experimental Epilepsy, UCL Institute of Neurology, London, UK
65 Chalfont Centre for Epilepsy, Bucks, UK

Correspondence to: Sanjay M. Sisodiya
Department of Clinical and Experimental Epilepsy
UCL Institute of Neurology
Box 29
Queen Square
London WC1N 3BG, UK
E-mail: s.sisodiya@ucl.ac.uk

Introduction

Epilepsy is a prevalent neurological disorder, comprising many different syndromes and conditions, affecting 0.6–1.5% of the population worldwide (Bell et al., 2014). Approximately one-third of affected individuals do not respond to antiepileptic drug therapy (French, 2007). Alternative treatment options may not be appropriate (Englot et al., 2011), and are not always effective (Téllez-Zenteno et al., 2005; Englot et al., 2011). The identification of shared biological disease pathways may help elucidate diagnostic and prognostic biomarkers and therapeutic targets, which, in turn, could help to optimize individual treatment (Pitkänen et al., 2016). However, disease biology remains unexplained for most cases—especially in commonly occurring epilepsies.

Epilepsy is a network disorder typically involving widespread structural alterations beyond the putative epileptic focus (Bernhardt et al., 2015; Vaughan et al., 2016). Hippocampal sclerosis is a common pathological substrate of mesial temporal lobe epilepsy (MTLE), but extrahippocampal abnormalities are also frequently observed in MTLE, notably in the thalamus (Keller and Roberts, 2008; Coan et al., 2014; Alvim et al., 2016) and neocortex (Keller and Roberts, 2008; Bernhardt et al., 2009b, 2010; Blanc et al., 2011; Labate et al., 2011; Vaughan et al., 2016). Neocortical abnormalities are also reported in idiopathic generalized epilepsies (IGE) (Bernhardt et al., 2009a), and many childhood syndromes (O'Muircheartaigh et al., 2011; Vollmar et al., 2011; Ronan et al., 2012; Overvliet et al., 2013). Thus, common epilepsies may be characterized by shared disturbances in distributed cortico-subcortical

brain networks (Berg *et al.*, 2010), but the pattern, consistency and cause of these disturbances, and how they relate to functional decline (Vlooswijk *et al.*, 2010; Bernasconi, 2016; Nickels *et al.*, 2016), are largely unknown.

Currently, we lack reliable data from large cross-sectional neuroimaging, brain tissue, or biomarker studies in the common epilepsies. Brain tissue is not available from large cohorts of patients: common forms of epilepsy are often unsuitable for surgical treatment, so biopsied tissues are simply unavailable in sufficient numbers for research into disease biology. Brain-wide post-mortem studies also require extensive effort for comprehensive analysis. MRI offers detailed information on brain structure, but MRI measures from groups of individuals with and without epilepsy are not always consistent. For example, MTLE is associated with hippocampal sclerosis in up to 70% of brain MRI scans (Blümcke *et al.*, 2013). However, the effects of laterality, and the extent of extrahippocampal grey matter loss are inconsistently reported in studies of left versus right MTLE (Kemmotsu *et al.*, 2011; Liu *et al.*, 2016). Similarly, abnormalities of the basal ganglia, hippocampus, lateral ventricles, and neocortex have all been reported in IGE (Betting *et al.*, 2006), but most alterations are non-specific, and visual inspection of clinical MRI in IGE is typically normal (Woermann *et al.*, 1998). Genome-wide association studies (GWAS) have identified genetic variants associated with complex epilepsies by 'lumping' different epilepsy types together (International League Against Epilepsy Consortium on Complex Epilepsies, 2014), but MRI studies are typically of smaller scale, and have not widely explored whether distinct epilepsy syndromes share common structural abnormalities.

There are many sources of inconsistency in previously reported MRI findings. First, epileptic seizures and syndromes are diverse; classifications are often revised and contested (Berg *et al.*, 2010; Scheffer *et al.*, 2017). Second, most cross-sectional brain imaging studies are based on small samples (typically <50 cases), limiting the power to detect subtle group differences (Button *et al.*, 2013). Third, variability in scanning protocols, image processing, and statistical analysis may affect the sensitivity of brain measures across studies.

The Enhancing Neuro Imaging Genetics through Meta-Analysis (ENIGMA) Consortium was formed to address these issues (Bearden and Thompson, 2017). ENIGMA is a global initiative, combining large samples with coordinated image processing, and integrating genomic and MRI data across hundreds of research centres worldwide. Prior ENIGMA studies have identified genetic variants associated with variations in brain structure (Stein *et al.*, 2012; Hibar *et al.*, 2015, 2017*a*; Adams *et al.*, 2016), and have reliably characterized patterns of brain abnormalities in schizophrenia (van Erp *et al.*, 2016), major depression (Schmaal *et al.*, 2016), obsessive compulsive disorder (Boedhoe *et al.*, 2017), attention deficit hyperactivity disorder (Hoogman *et al.*, 2017), and many other brain illnesses (Thompson *et al.*, 2017). Large-scale, collaborative

initiatives such as ENIGMA may improve our understanding of epilepsy, helping clinicians make more informed decisions and provide personalized treatment strategies (Ben-Menachem, 2016). Thus, we formed the Epilepsy Working Group of ENIGMA ('ENIGMA-Epilepsy') to apply coordinated, well-powered studies of imaging and genetic data in epilepsy.

Here, in the largest analysis of structural brain abnormalities in epilepsy to date, we ranked effect sizes for 16 subcortical and 68 cortical brain regions in 2149 individuals with epilepsy and 1727 healthy controls, using harmonized image processing, quality control, and meta-analysis. First, we grouped all epilepsies together, to determine whether biologically distinct syndromes show robust, common structural deficits. Second, we assessed a well-characterized form of epilepsy: MTLE with hippocampal sclerosis, analysing patients with left- and right-sided hippocampal sclerosis as independent groups. Third, we examined another major set of epilepsy syndromes: IGE. Finally, we studied all remaining epilepsies as a combined subgroup, to understand the relative contributions of IGE, MTLE-L, MTLE-R, and all other syndromes on shared patterns of structural compromise. We tested how age at scan, age of onset, and epilepsy duration affected brain structural measures. Based on existing neuroimaging (Gotman *et al.*, 2005; Bernhardt *et al.*, 2009*a*; Liu *et al.*, 2016), neurophysiological (Gotman *et al.*, 2005), neuropathological (Thom *et al.*, 2009), and genetic data (International League Against Epilepsy Consortium on Complex Epilepsies, 2014), we predicted that (i) biologically distinct epilepsy syndromes would exhibit shared patterns of structural abnormalities; (ii) MTLEs with left or right hippocampal sclerosis would show distinct patterns of hippocampal and extrahippocampal structural deficits; and (iii) IGEs would also display subcortical volume and cortical thickness differences, compared to healthy controls.

Materials and methods

Each centre received approval from their local institutional review board or ethics committee. Written informed consent was provided according to local requirements (Supplementary Table 1).

Experimental design

Participants

Twenty-four cross-sectional samples from 14 countries were included in the study, totalling 2149 people with epilepsy and 1727 research centre-matched healthy control subjects (Fig. 1 and Table 1). The locations, dates, and periods of participant recruitment are provided in Supplementary Table 1. An epilepsy specialist assessed seizure and syndrome classifications at each centre, using International League Against Epilepsy terminology (Berg *et al.*, 2010). Participants were aged 18–55.

To test for shared and syndrome-specific structural alterations, analyses included one group combining all epilepsies ('all-epilepsies'; $n = 2149$), and four stratified subgroups: (i) left MTLE with left hippocampal sclerosis (MTLE-L; $n = 415$); (ii) right MTLE with right hippocampal sclerosis (MTLE-R; $n = 339$); (iii) IGE ($n = 367$); and (iv) all other epilepsies ($n = 1028$). Supplementary Table 2 lists all syndromic diagnoses included in the aggregate 'all-epilepsies' group. For the MTLE subgroups, we included anyone with the typical electroclinical constellation (Berg *et al.*, 2010), and a neuroradiologically-confirmed diagnosis of unilateral hippocampal sclerosis on clinical MRI. Participants were included in the IGE subgroup if they presented with tonic-clonic, absence or myoclonic seizures with generalized spike-wave discharges on EEG. Participants were included in the 'all-other-epilepsies' subgroup if they were diagnosed with non-lesional MTLE (43.3%), occipital (1.67%), frontal (8.78%), or parietal lobe epilepsy (0.84%), focal epilepsies not otherwise specified (37.03%), or another unclassified syndrome (8.37%; Supplementary Table 2). We excluded participants with a progressive disease (e.g. Rasmussen's encephalitis), malformations of cortical development, tumours or previous neurosurgery.

MRI data collection and processing

Structural T$_1$-weighted MRI brain scans were collected at the 24 participating centres. Scanning details are provided in Supplementary Table 3. T$_1$-weighted images from cases and controls were analysed at each site using FreeSurfer 5.3.0, for automated analysis of brain structure (Fischl, 2012). Volumetric measures were extracted for 12 subcortical grey matter regions (six left and six right, including the amygdala, caudate, nucleus accumbens, pallidum, putamen, and thalamus), the left and right hippocampi, and the left and right lateral ventricles. Cortical thickness measures were extracted for 34 left-hemispheric grey matter regions, and 34 right-hemispheric grey matter regions (68 total; Supplementary Table 4). Visual inspections of subcortical and cortical segmentations were conducted following standardized ENIGMA protocols (http://enigma.usc.edu), used in prior genetic studies of brain structure (Stein *et al.*, 2012; Hibar *et al.*, 2015, 2017*a*; Adams *et al.*, 2016), and large-scale case-control studies of neuropsychiatric illnesses (Schmaal *et al.*, 2015, 2016; Hibar *et al.*, 2016; van Erp *et al.*, 2016; Boedhoe *et al.*, 2017). Analysts were blind to participants' diagnoses. Each analyst was instructed to execute a series of standardized bash scripts, identifying participants with volumetric or thickness measures greater or less than 1.5 times the interquartile range as outliers. Outlier data were then visually inspected, by overlaying the participant's cortical segmentations on their whole-brain anatomical images. If the blinded local analyst judged any structure as inaccurately segmented, that structure was omitted from the analysis. The Supplementary material provides further information.

Statistical analysis

Participant demographics

All research centres tested for differences in age between individuals with epilepsy and controls using an unpaired, two-tailed *t*-test in the *R* statistics package (https://www.r-project.org). Each centre also tested for sex differences between individuals with epilepsy and controls using a chi-squared test in SPSS Statistics package (IBM Corp., Version 21.0).

Meta-analytical group comparisons

Each research centre tested for case-versus-control differences using multiple linear regressions (via the *lm* function implemented in *R*), where a binary indicator of diagnosis (0 = healthy control, 1 = person with epilepsy) was the predictor of interest, and the volume or thickness of a specified brain region was the outcome measure. We calculated effect size estimates across all brain regions using Cohen's *d*, adjusting for age, sex and intracranial volume (ICV). ICV is a reliable, indirect measure of head size (Hansen *et al.*, 2015), used as a covariate in other large-scale ENIGMA collaborations (Schmaal *et al.*, 2015, 2016; Hibar *et al.*, 2016; van Erp *et al.*, 2016; Boedhoe *et al.*, 2017). Cohen's *d* effect sizes and regression beta coefficients were pooled across centres using a random-effects, restricted maximum likelihood method of meta-analysis via the *R* package, *metafor* (Viechtbauer, 2010). The Supplementary material provides additional details.

Meta-analytical regression with clinical variables

Each centre conducted a series of linear regressions, testing the association between subcortical volume or cortical thickness, and: (i) age at onset of epilepsy; and (ii) duration of epilepsy.
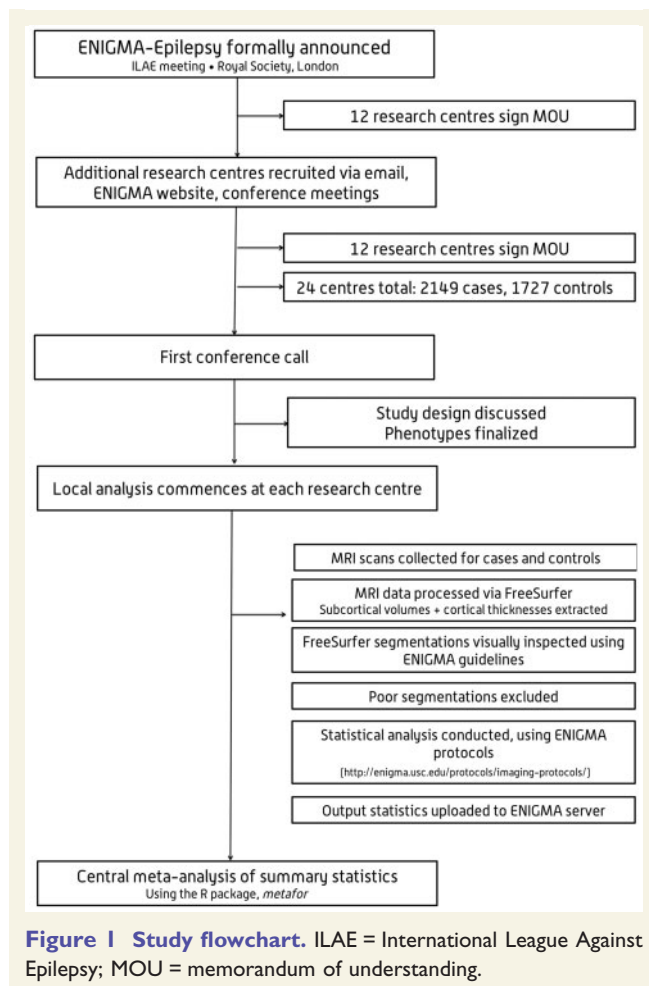

Figure 1 Study flowchart. ILAE = International League Against Epilepsy; MOU = memorandum of understanding.

Table 1 ENIGMA - Epilepsy Working Group demographics, including age (in years), mean age at onset of epilepsy (in years), mean duration of illness (in years), sex, and case-control breakdown for participating sites

Site name	Age controls (Mean ± SD)	Age cases (Mean ± SD)	Age of onset (Mean ± SD)	Duration of illness (Mean ± years)	Female controls	Female cases	Total controls	Total cases	MTLE-L cases	MTLE-R cases	IGE cases	'Other' cases	Total n
Bern	32.5 ± 9.39	30.48 ± 10.13	-	-	41	28	78	56	10	8	12	26	134
Bonn	40.11 ± 13.4	39.68 ± 13.4	16.86 ± 11.96	22.82 ± 14.18	40	60	77	108	71	37	0	0	185
BRI	34.73 ± 10.61	33.28 ± 10.59	17.9 ± 11.49	17.9 ± 12.93	49	46	112	79	10	13	18	38	191
Brussels	26.64 ± 4.34	33.79 ± 9.9	14.46 ± 10.13	19.02 ± 12.77	24	49	44	83	11	0 (4)	8	60	127
CUBRIC	28.04 ± 8.16	28.42 ± 8.06	13.56 ± 5.18	14.81 ± 9.91	34	34	48	48	0	0	44	0 (4)	96
EKUT_A	34.82 ± 11.38	33.58 ± 11.07	17.04 ± 11.09	16.84 ± 13.18	30	28	49	47	6	0	5	36	96
EKUT_B	35.33 ± 12.27	31.13 ± 10.74	17.32 ± 10.8	14.45 ± 11.14	9	18	18	24	0	0	16	8	42
EPICZ	30.48 ± 9.39	30.42 ± 10.13	-	-	59	71	116	113	19	27	0	67	229
EPIGEN_3.0	34.75 ± 9.36	36.2 ± 9.97	17.03 ± 13.7	18.93 ± 10.88	30	37	70	60	8	5	0	47	130
EPIGEN_1.5	31.7 ± 9.24	37.46 ± 10.69	14.51 ± 11.8	22.68 ± 14.28	24	35	47	52	27	25	0	0	99
Florence	35.29 ± 8.48	28 ± 7.77	12.69 ± 8.02	14.27 ± 8.06	8	12	14	31	0 (1)	0	5	25	45
Greifswald	42.26 ± 14.97	26.23 ± 7.49	28.12 ± 17.86	14.13 ± 12.81	60	21	99	39	0	0	39	0	138
IDIBAPS-HCP	33.13 ± 5.99	36.77 ± 9.52	18.07 ± 11.72	17.64 ± 10.51	29	67	52	115	17	36	0 (3)	59	167
KCL_CNS	31.68 ± 8.4	33.2 ± 8.9	13.22 ± 8.2	20.67 ± 11.23	54	50	101	96	5	0 (4)	32	55	197
KCL_CRF	28.73 ± 8.29	31.47 ± 11.33	23.13 ± 7.55	8.33 ± 9.99	16	7	26	15	0 (3)	0 (2)	0 (4)	6	41
Kuopio	25.16 ± 1.55	33.35 ± 11.21	24 ± 13.22	9.35 ± 11.23	33	135	67	240	0	9	36	195	307
MNI	30.74 ± 7.38	32.53 ± 9.92	16.48 ± 9.72	16.05 ± 11.32	21	71	46	128	45	38	0	45	174
NYU	30.1 ± 10.36	33.23 ± 9.66	16.96 ± 11.27	16.43 ± 12.7	62	93	118	159	8	11	36	104	277
RMH	39.35 ± 20.26	38.08 ± 15.91	28.23 ± 17.98	10.18 ± 12.65	12	70	28	146	22	13	25	86	174
UCSD	36.89 ± 15.1	37.67 ± 11.79	19.32 ± 14.77	18.8 ± 15.36	16	22	37	43	14	8	0	21	80
UNAM	33.2 ± 12.29	31.47 ± 11.81	16.26 ± 11.33	15.03 ± 12.53	25	24	35	36	10	10	0	16	71
UNICAMP	34.39 ± 10.45	39.98 ± 10.25	12.07 ± 9.52	27.96 ± 12.54	249	183	398	291	107	84	40	60	689
UNIMORE	28.47 ± 5.25	28.36 ± 0.26	12.58 ± 8.13	14.34 ± 0.94	20	47	34	82	0 (3)	0 (2)	40	37	116
XMU	31.54 ± 6.99	28.79 ± 9.06	17.04 ± 12.2	11.76 ± 8.78	4	20	13	58	25	15	11	7	71
Combined	33.31 ± 9.91	34.36 ± 10.65	17.63 ± 11.47	17.42 ± 11.99	949	1228	1727	2149	415	339	367	1028	3876

Also provided is the total number of MTLE cases. MTLE cases with left hippocampal sclerosis, MTLE cases with right hippocampal sclerosis, IGE and all-other-epilepsies ('other') cases per site. Research centres with fewer than five participants for a given phenotype are marked as '0' for that phenotype, with the original sample size noted in parentheses.
SD = standard deviation.

All centres tested for interactions between diagnosis of epilepsy (including syndrome groups) and age at time of scan. Beta values representing the unstandardized slopes of each regression were extracted for each analysis. Sex and ICV were included as covariates in all secondary analyses.

Correction for multiple comparisons

We conducted four independent regressions (one case versus control regression, and three regressions with clinical variables) across 84 regions of interest, adjusting the statistical significance threshold to $P_{thresh} < 1.49 \times 10^{-4}$ to correct for 336 comparisons. To account for correlations between tests, we also applied a less conservative adjustment for false discovery rate (FDR), using the Benjamini and Hochberg method (Benjamini and Hochberg, 1995). For clarity, we report only P-values significant after stringent Bonferroni correction; FDR-adjusted P-values are summarized in the Supplementary material.

Power analyses

Across all regions of interest, we calculated the sample sizes necessary to achieve 80% power to detect case-control differences, given the observed effect sizes at each region of interest, based on two-tailed t-tests, using G*Power Version 3.1. For each region of interest, we also estimated N_{80}: the total number of samples required, per group, to achieve 80% power to detect group differences using a t-test at the threshold of $P < 0.05$ (two-tailed).

Results

Participant demographics

The sample size-weighted mean age across all epilepsy samples was 34.4 (range: 26.2–40) years, and the weighted mean age of healthy controls was 33.3 (range: 25.2–42.3) years. The weighted mean age at onset of epilepsy and duration of epilepsy were 17.6 (range: 12.1–28.2) years and 17.4 (range: 8.3–28) years, respectively. Females comprised 57% of the total epilepsy sample (range: 34–75% by individual sample), and 53% of the controls (range: 31–71% by individual sample). Case-control differences in age were observed at 8 of 24 research centres, and case-control differences in sex were observed at 2 of 24 research centres (Supplementary Table 5); hence, age and sex were included as covariates in all group comparisons.

Volumetric findings

Compared to controls, the aggregate all-epilepsies group exhibited lower volumes in the left ($d = -0.36$; $P = 1.31 \times 10^{-6}$) and right thalamus ($d = -0.37$; $P = 7.67 \times 10^{-14}$), left ($d = -0.35$; $P = 3.04 \times 10^{-7}$) and right hippocampus ($d = -0.34$; $P = 6.63 \times 10^{-10}$), and the right pallidum ($d = -0.32$; $P = 8.32 \times 10^{-9}$). Conversely, the left ($d = 0.29$; $P = 2.14 \times 10^{-12}$) and right ($d = 0.27$; $P = 3.73 \times 10^{-15}$) lateral ventricles were enlarged across all epilepsies when compared to controls (Table 2 and Fig. 2A). A supplementary analysis of all-epilepsies,

excluding individuals with hippocampal sclerosis or other lesions, revealed similar patterns of volume loss in the right thalamus and pallidum, and bilaterally enlarged ventricles; however, volume differences were not observed in the hippocampus (Supplementary Table 6).

The MTLE-L subgroup showed lower volumes in the left hippocampus ($d = -1.73$; $P = 1.35 \times 10^{-19}$), left ($d =$ $P = 2.19 \times 10^{-11}$) and right thalamus ($d = -0.46$; $P = 8.12 \times 10^{-5}$), left putamen ($d = -0.39$; $P = 1.07 \times 10^{-6}$), and right pallidum ($d = -0.45$; $P = 5.48 \times 10^{-7}$). As in the overall group comparison, we observed larger left ($d = 0.47$; $P = 1.96 \times 10^{-7}$) and right lateral ventricles ($d = 0.36$; $P = 8.95 \times 10^{-5}$) in MTLE-L patients relative to controls (Table 2 and Fig. 2B).

The MTLE-R subgroup showed lower volumes across a number of regions in the right hemisphere only, including the hippocampus ($d = -1.91$; $P = 6.36 \times 10^{-37}$), thalamus ($d = -0.73$; $P = 1.6 \times 10^{-12}$), and pallidum ($d = -0.45$; $P = 3.96 \times 10^{-7}$), together with increased volumes of the left ($d = 0.39$; $P = 1.52 \times 10^{-6}$) and right lateral ventricles ($d = 0.44$; $P = 6.57 \times 10^{-12}$) compared to controls (Table 2 and Fig. 2C).

The IGE subgroup showed lower volumes in the right thalamus ($d = -0.4$; $P = 3.6 \times 10^{-6}$) compared to controls (Table 2 and Fig. 2D).

The all-other-epilepsies subgroup showed lower volumes in the right thalamus ($d = -0.31$; $P = 7.9 \times 10^{-11}$) and the right pallidum ($d = -0.24$; $P = 8.1 \times 10^{-5}$) compared to controls. The all-other-epilepsies subgroup also showed significant enlargements of the left ($d = 0.33$; $P = 5.1 \times 10^{-7}$) and right amygdala ($d = 0.22$; $P = 1.46 \times 10^{-4}$), and the left ($d = 0.2$; $P = 1.2 \times 10^{-5}$) and right lateral ventricles ($d = 0.21$; $P = 4.62 \times 10^{-6}$) compared to controls (Table 2 and Fig. 2E).

All volume differences can be visualized using the interactive ENIGMA-Viewer tool (Zhang et al., 2017), at http://enigma-viewer.org/ENIGMA_epilepsy_subcortical.html (Supplementary material). Volume differences significant after FDR adjustment can also be visualized at http://enigma-viewer.org/ENIGMA_epilepsy_subcortical_fdr.html (Supplementary Tables 26–30).

Cortical thickness findings

The all-epilepsies group showed reduced thickness of cortical grey matter across seven regions bilaterally, including the left ($d = -0.38$; $P = 1.82 \times 10^{-18}$) and right precentral gyri ($d = -0.4$; $P = 8.85 \times 10^{-20}$), left ($d = -0.32$; $P = 2.11 \times 10^{-15}$) and right caudal middle frontal gyri ($d = -0.31$; $P = 2.09 \times 10^{-9}$), left ($d = -0.31$; $P = 2.05 \times 10^{-6}$) and right paracentral gyri ($d = -0.32$; $P = 2.19 \times 10^{-9}$), left ($d = -0.19$; $P = 1.29 \times 10^{-4}$) and right pars triangularis ($d = -0.2$; $P = 4.25 \times 10^{-8}$), left ($d = -0.28$; $P = 1.51 \times 10^{-7}$) and right superior frontal gyri ($d = -0.27$; $P = 4.49 \times 10^{-6}$), left ($d = -0.19$; $P = 1.05 \times 10^{-5}$) and right transverse temporal gyri ($d = -0.18$; $P = 2.81 \times 10^{-5}$), and left ($d = -0.23$; $P = 9.87 \times 10^{-5}$) and right

Table 2 Effect size differences between epilepsy cases and healthy controls (Cohen's d) for the mean volume of subcortical structures, controlling for age, sex and intracranial volume

Structure	Phenotype	Cohen's d	SE	Z score	95% CI	P-value	I^2	N_{80}	Number of controls	Number of cases
Amygdala (LH)	All-other-epilepsies	0.327	0.065	5.024	0.199–0.455	5.05×10^{-7}	45.470	148	1448	998
Amygdala (RH)	All-other-epilepsies	0.218	0.057	3.799	0.106–0.33	1.46×10^{-4}	31.256	335	1422	989
Hippocampus (LH)	MTLE-L	−1.728	0.191	−9.056	−2.102 to −1.354	1.35×10^{-19}	85.532	7	1412	410
	All epilepsies	−0.353	0.069	−5.121	−0.488 to −0.217	3.04×10^{-7}	71.845	127	1707	2125
Hippocampus (RH)	MTLE-R	−1.906	0.15	−12.694	−2.2 to −1.611	6.36×10^{-37}	72.476	6	1286	336
	All epilepsies	−0.336	0.054	−6.175	−0.443 to −0.229	6.63×10^{-10}	54.801	141	1719	2129
Lateral ventricle (LH)	MTLE-L	0.465	0.089	5.203	0.289–0.640	1.96×10^{-7}	43.124	74	1417	414
	MTLE-R	0.39	0.081	4.808	0.231–0.549	1.52×10^{-6}	26.750	105	1291	338
	All epilepsies	0.288	0.041	7.025	0.207–0.368	2.14×10^{-12}	23.338	191	1722	2135
	All-other-epilepsies	0.198	0.045	4.373	0.109–0.287	1.23×10^{-5}	0.218	402	1452	996
Lateral ventricle (RH)	MTLE-R	0.444	0.065	6.867	0.317–0.57	6.57×10^{-12}	0.003	81	1292	338
	MTLE-L	0.363	0.093	3.917	0.1814–0.544	8.95×10^{-5}	47.227	121	1418	414
	All epilepsies	0.268	0.034	7.864	0.2–0.334	3.73×10^{-15}	0	220	1722	2137
	All-other-epilepsies	0.212	0.046	4.581	0.122–0.303	4.62×10^{-6}	3.528	350	1453	996
Pallidum (RH)	MTLE-L	−0.452	0.09	−5.009	−0.628 to −0.275	5.48×10^{-7}	43.985	78	1406	414
	MTLE-R	−0.451	0.089	−5.071	−0.624 to −0.276	3.96×10^{-7}	36.432	79	1278	332
	All epilepsies	−0.316	0.055	−5.762	−0.424 to −0.208	8.32×10^{-9}	55.575	159	1710	2112
	All-other-epilepsies	−0.235	0.060	−3.942	−0.352 to −0.118	8.07×10^{-5}	36.141	286	1440	976
Putamen (LH)	MTLE-L	−0.385	0.079	−4.878	−0.539 to −0.23	1.07×10^{-6}	28.474	107	1352	410
Thalamus (LH)	MTLE-L	−0.843	0.126	−6.693	−1.089 to −0.595	2.19×10^{-11}	70.462	24	1384	408
	All epilepsies	−0.358	0.074	−4.839	−0.503 to −0.213	1.31×10^{-6}	75.649	124	1687	2104
Thalamus (RH)	MTLE-R	−0.727	0.103	−7.066	−0.928 to −0.525	1.60×10^{-12}	51.499	31	1285	335
	MTLE-L	−0.462	0.117	−3.941	−0.691 to −0.232	8.12×10^{-5}	67.376	75	1412	414
	IGE	−0.403	0.087	−4.633	−0.574 to −0.233	3.60×10^{-6}	39.715	98	1210	363
	All epilepsies	−0.368	0.049	−7.476	−0.464 to −0.271	7.67×10^{-14}	44.822	117	1716	2137
	All-other-epilepsies	−0.305	0.047	−6.502	−0.397 to −0.213	7.92×10^{-11}	4.985	170	1446	998

CI = confidence interval; LH = left hemisphere; RH = right hemisphere; SE = standard error; I^2 = heterogeneity index; N_{80} = number of subjects required in each group to yield 80% power to detect significant group differences ($P < 0.05$, two-tailed). Uncorrected P-values are reported. Subcortical structures that failed to survive Bonferroni correction ($P < 1.49 \times 10^{-4}$) are not reported (see 'Materials and methods' section for statistical threshold determination). See Supplementary material for a full list of volume differences with adjustment for false discovery rate (FDR).
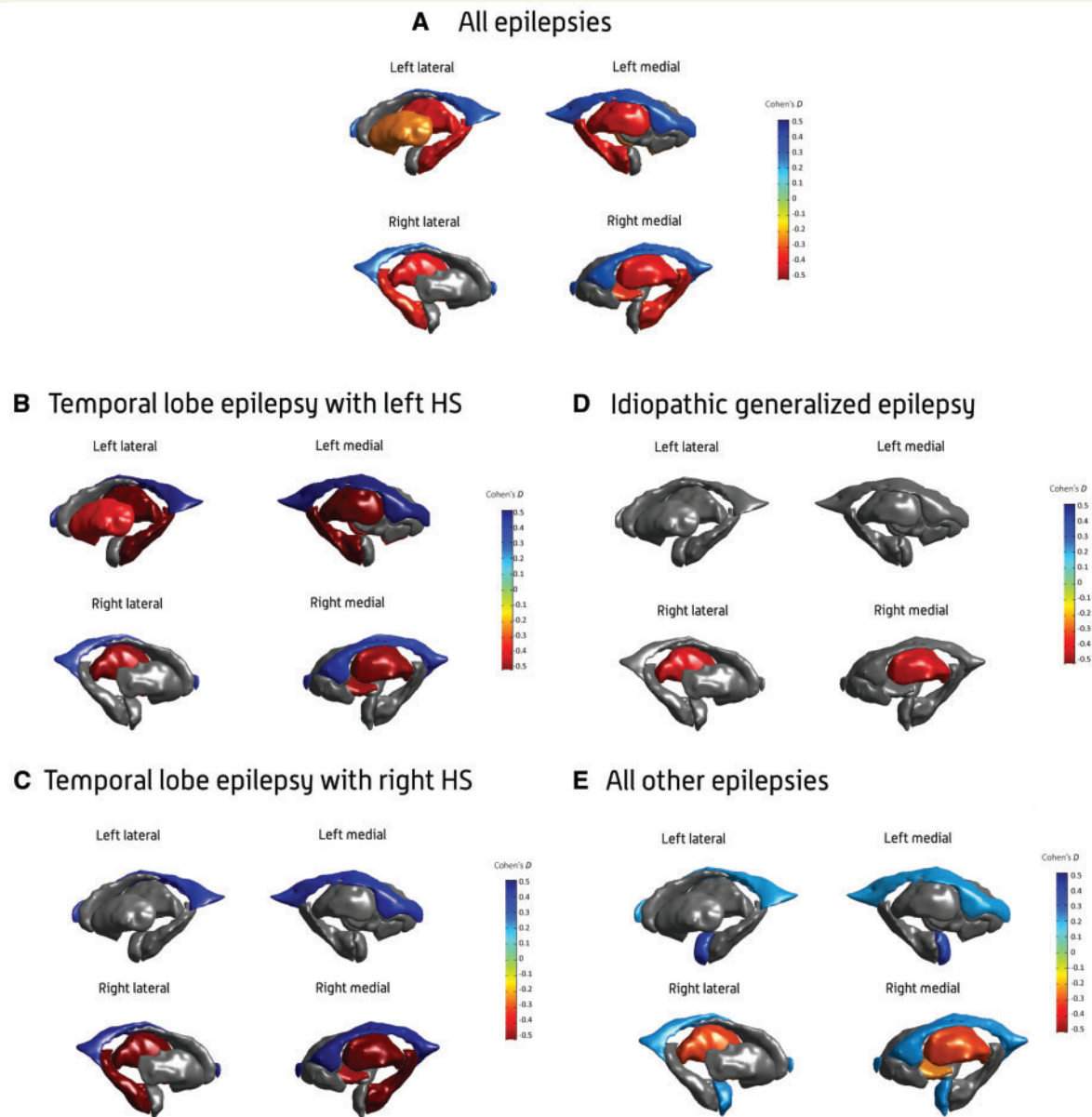
Figure 2 Subcortical volume findings. Cohen's *d* effect size estimates for case-control differences in subcortical volume, across the (**A**) all-epilepsies, (**B**) mesial temporal lobe epilepsies with left hippocampal sclerosis (HS; MTLE-L), (**C**) mesial temporal lobe epilepsies with right hippocampal sclerosis (MTLE-R), (**D**) idiopathic generalized epilepsies (IGE), and (**E**) all-other-epilepsies groups. Cohen's *d* effect sizes were extracted using multiple linear regressions, and pooled across research centres using random-effects meta-analysis. Subcortical structures with *P*-values < 1.49×10^{-4} are shown in heatmap colours; strength of heat map is determined by the size of the Cohen's *d* (*d* < 0 = blue, *d* > 0 = yellow/red). Image generated using MATLAB, with annotations added using Adobe Photoshop. An interactive version of this figure is available online, via 'ENIGMA-Viewer': http://enigma-viewer.org/ENIGMA_epilepsy_subcortical.html. See Supplementary material for guidelines on how to use the interactive visualization.

supramarginal gyri (*d* = −0.22; *P* = 5.24×10^{-5}). The all-epilepsies group also showed unilaterally thinner right cuneus (*d* = −0.2; *P* = 9.68×10^{-8}), right pars opercularis (*d* = −0.18; *P* = 6.48×10^{-7}), right precuneus (*d* = −0.28; *P* = 2.7×10^{-5}), and left entorhinal gyrus (*d* = −0.26; *P* = 2.04×10^{-5}), compared to healthy controls (Table 3 and Fig. 3A). Supplementary analysis in a non-lesional epilepsy subgroup revealed a similar pattern of cortical thickness differences compared to controls, suggesting that the

changes observed in our main analysis were not driven by the inclusion of patients with hippocampal sclerosis or other common lesions (Supplementary Table 7).

The MTLE-L and MTLE-R subgroups showed distinct patterns of cortical thickness reductions when compared to healthy controls (Table 3, Fig. 3B and C). In MTLE-R, lower cortical thickness was reported across four motor regions, including the left (*d* = −0.51; *P* = 7.67×10^{-7}) and right paracentral gyri (*d* = −0.42; *P* = 6.24×10^{-11}),

Table 3 Effect size differences between epilepsy cases and healthy controls (Cohen's *d*) for the mean thickness of cortical structures, controlling for age, sex and intracranial volume

Structure	Phenotype	Cohen's *d*	SE	Z score	95% CI	P-value	I^2	N_{80}	Number of controls	Number of cases
Caudal middle frontal gyrus (LH)	MTLE-L	−0.403	0.07	−5.789	−0.538 to −0.2663	7.07×10^{-9}	13.807	98	1344	412
	All epilepsies	−0.319	0.04	−7.935	−0.397 to −0.24	2.11×10^{-15}	17.112	156	1650	2061
	All other epilepsies	−0.291	0.045	−6.425	−0.38 to −0.202	1.32×10^{-10}	0	197	1447	1000
Caudal middle frontal gyrus (RH)	MTLE-L	−0.441	0.087	−5.089	−0.611 to −0.271	3.61×10^{-7}	39.444	82	1348	412
	All epilepsies	−0.307	0.051	−5.991	−0.407 to −0.206	2.09×10^{-9}	46.443	168	1653	2059
	All other epilepsies	−0.212	0.045	−4.699	−0.301 to −0.124	2.62×10^{-6}	0	350	1451	998
Cuneus (RH)	All other epilepsies	−0.234	0.045	−5.186	−0.323 to −0.146	2.15×10^{-7}	0	288	1449	996
	All epilepsies	−0.204	0.038	−5.333	−0.279 to −0.129	9.68×10^{-8}	11.423	379	1651	2057
Entorhinal gyrus (LH)	MTLE-L	−0.445	0.072	−6.158	−0.5865 to −0.303	7.35×10^{-10}	0	81	1102	303
	All epilepsies	−0.264	0.062	−4.261	−0.385 to −0.142	2.04×10^{-5}	56.648	227	1402	1724
Fusiform gyrus (LH)	MTLE-L	−0.359	0.069	−5.183	−0.494 to −0.223	2.19×10^{-7}	13.465	123	1339	412
Lateral occipital gyrus (RH)	All other epilepsies	−0.211	0.045	−4.659	−0.299 to −0.122	3.18×10^{-6}	2.50×10^{-3}	354	1450	997
Lingual gyrus (RH)	All other epilepsies	−0.180	0.045	−3.972	−0.268 to −0.091	7.12×10^{-5}	1.25×10^{-2}	491	1450	996
Paracentral gyrus (LH)	MTLE-R	−0.505	0.102	−4.944	−0.705 to −0.305	7.67×10^{-7}	52.283	63	1292	338
	MTLE-L	−0.426	0.099	−4.313	−0.62 to −0.232	1.61×10^{-5}	53.165	88	1344	412
	All epilepsies	−0.311	0.065	−4.748	−0.439 to −0.182	2.05×10^{-6}	67.476	164	1650	2061
	All other epilepsies	−0.257	0.045	−5.680	−0.346 to −0.168	1.34×10^{-8}	0	239	1447	1000
Paracentral gyrus (RH)	MTLE-R	−0.421	0.064	−6.538	−0.548 to −0.295	6.24×10^{-11}	0.407	90	1296	338
	MTLE-L	−0.378	0.075	−5.021	−0.526 to −0.231	5.14×10^{-7}	23.536	111	1348	412
	All other epilepsies	−0.351	0.045	−7.733	−0.44 to −0.262	1.05×10^{-14}	3.43×10^{-3}	129	1451	998
	All epilepsies	−0.315	0.053	−5.983	−0.418 to −0.212	2.19×10^{-9}	49.261	160	1654	2059
Parahippocampal gyrus (LH)	MTLE-L	−0.3	0.073	−4.11	−0.444 to −0.1572	3.95×10^{-5}	19.366	176	1335	410
Pars opercularis (RH)	MTLE-R	−0.271	0.071	−3.8	−0.411 to −0.131	1.45×10^{-4}	12.105	215	1295	338
	All epilepsies	−0.177	0.036	−4.976	−0.247 to −0.107	6.48×10^{-7}	2.624	503	1652	2059
Pars triangularis (LH)	All epilepsies	−0.192	0.05	−3.828	−0.2897 to −0.094	1.29×10^{-4}	44.414	427	1650	2060
Pars triangularis (RH)	MTLE-L	−0.285	0.06	−4.738	−0.403 to −0.167	2.16×10^{-6}	0	195	1346	412
	All epilepsies	−0.199	0.036	−5.48	−0.27 to −0.128	4.25×10^{-8}	4.66	398	1652	2058
	All other epilepsies	−0.210	0.045	−4.650	−0.299 to −0.122	3.32×10^{-6}	2.58×10^{-3}	357	1449	998
Precentral gyrus (LH)	MTLE-L	−0.466	0.081	−5.755	−0.625 to −0.307	8.64×10^{-9}	31.602	74	1339	412
	MTLE-R	−0.415	0.09	−4.596	−0.592 to −0.238	4.31×10^{-6}	40.044	93	1287	338
	All epilepsies	−0.384	0.044	−8.768	−0.469 to −0.298	1.82×10^{-18}	27.649	108	1645	2058
	All other epilepsies	−0.375	0.046	−8.237	−0.464 to −0.286	1.76×10^{-16}	5.59×10^{-3}	113	1442	997
	IGE	−0.342	0.071	−4.78	−0.482 to −0.201	1.75×10^{-6}	0.003	136	1043	297
Precentral gyrus (RH)	MTLE-R	−0.52	0.086	−6.073	−0.687 to −0.352	1.25×10^{-9}	33.288	60	1293	337
	MTLE-L	−0.492	0.078	−6.335	−0.6436 to −0.339	2.37×10^{-10}	26.33	66	1345	412
	All epilepsies	−0.399	0.044	−9.102	−0.485 to −0.313	8.85×10^{-20}	27.929	100	1649	2054
	IGE	−0.39	0.072	−5.442	−0.531 to −0.25	5.27×10^{-8}	0.005	105	1044	295
	All other epilepsies	−0.348	0.045	−7.672	−0.437 to −0.259	1.70×10^{-14}	0	131	1448	996
Precuneus (LH)	MTLE-L	−0.536	0.135	−3.965	−0.801 to −0.271	7.35×10^{-5}	75.18	56	1343	412
	All other epilepsies	−0.178	0.047	−3.819	−0.27 to −0.087	1.34×10^{-4}	4.474	497	1446	998

(continued)

Table 3 Continued

Structure	Phenotype	Cohen's d	SE	Z score	95% CI	P-value	I^2	N_{80}	Number of controls	Number of cases
Precuneus (RH)	MTLE-L	−0.473	0.104	−4.558	−0.676 to −0.27	5.16×10^{-6}	57.498	72	1348	412
	All epilepsies	−0.275	0.066	−4.197	−0.404 to −0.147	2.70×10^{-5}	67.608	209	1654	2055
	All other epilepsies	−0.238	0.053	−4.471	−0.343 to −0.134	7.78×10^{-6}	22.378	279	1451	994
Superior frontal gyrus (LH)	MTLE-L	−0.411	0.06	−6.804	−0.529 to −0.292	1.02×10^{-11}	0	94	1343	412
	All epilepsies	−0.283	0.054	−5.251	−0.389 to −0.177	1.51×10^{-7}	51.773	197	1649	2059
	All other epilepsies	−0.243	0.059	−4.138	−0.358 to −0.128	3.51×10^{-5}	34.545	267	1446	999
Superior frontal gyrus (RH)	MTLE-L	−0.365	0.06	−6.051	−0.483 to −0.246	1.44×10^{-9}	0	119	1345	412
	All epilepsies	−0.269	0.059	−4.588	−0.385 to −0.154	4.49×10^{-6}	59.483	218	1650	2058
	All other epilepsies	−0.235	0.052	−4.489	−0.337 to −0.132	7.15×10^{-6}	20.049	286	1448	997
Superior parietal gyrus (LH)	All other epilepsies	−0.224	0.045	−4.954	−0.313 to −0.136	7.27×10^{-7}	0.001	314	1444	996
Superior parietal gyrus (RH)	All other epilepsies	−0.220	0.045	−4.864	−0.309 to −0.131	1.15×10^{-6}	0.002	326	1450	997
Supramarginal gyrus (LH)	All epilepsies	−0.232	0.06	−3.894	−0.348 to −0.115	9.87×10^{-5}	59.391	293	1606	1965
Supramarginal gyrus (RH)	All epilepsies	−0.223	0.055	−4.045	−0.331 to −0.115	5.24×10^{-5}	52.895	317	1597	1971
	All other epilepsies	−0.206	0.047	−4.418	−0.297 to −0.115	9.95×10^{-6}	0	371	1395	961
Temporal pole (LH)	MTLE-L	−0.315	0.068	−4.649	−0.447 to −0.182	3.33×10^{-6}	10.901	160	1341	410
Transverse temporal gyrus (LH)	MTLE-R	−0.312	0.073	−4.249	−0.456 to −0.168	2.15×10^{-5}	15.614	163	1289	338
	All epilepsies	−0.192	0.044	−4.406	−0.278 to −0.107	1.05×10^{-5}	28.178	427	1647	2061
Transverse temporal gyrus (RH)	All epilepsies	−0.182	0.044	−4.188	−0.267 to −0.097	2.81×10^{-5}	27.918	475	1654	2059
	All other epilepsies	−0.18	0.045	−3.982	−0.269 to −0.091	6.84×10^{-5}	0.012	486	1451	998

CI = confidence interval; LH = left hemisphere; RH = right hemisphere; SE = standard error; I^2 = heterogeneity index; N_{80} = number of subjects required in each group to yield 80% power to detect significant group differences ($P < 0.05$, two-tailed). Uncorrected P-values are reported. Cortical regions that failed to survive Bonferroni correction ($P < 1.49 \times 10^{-4}$) are not reported (see 'Materials and methods' section for statistical threshold determination). See Supplementary material for a full list of cortical differences with adjustment for false discovery rate (FDR).
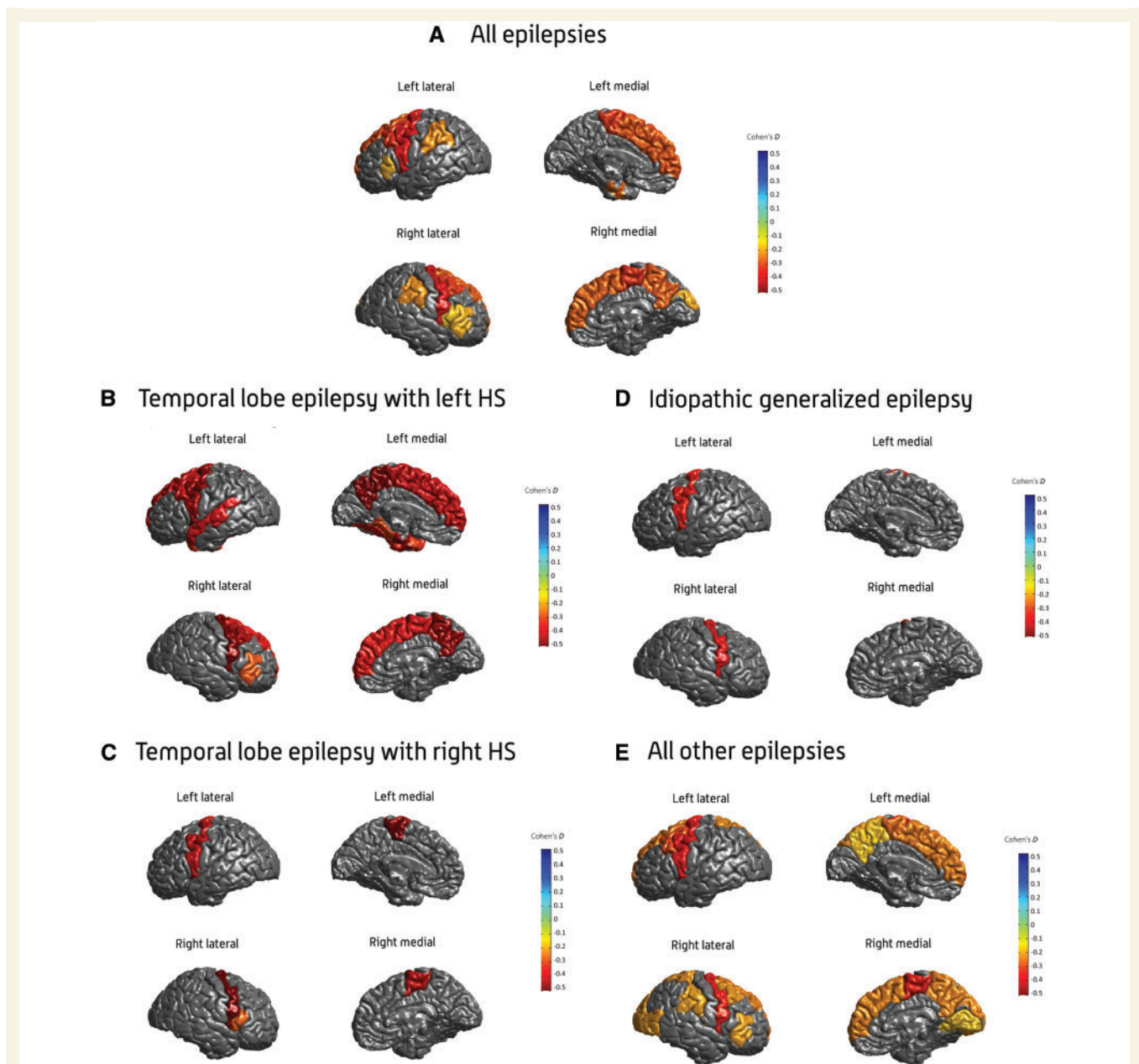
Figure 3 Cortical thickness findings. Cohen's *d* effect size estimates for case-control differences in cortical thickness, across the (**A**) all-epilepsies, (**B**) mesial temporal lobe epilepsies with left hippocampal sclerosis (MTLE-L), (**C**) mesial temporal lobe epilepsies with right hippocampal sclerosis (MTLE-R), (**D**) idiopathic generalized epilepsies (IGE), and (**E**) all-other-epilepsies groups. Cohen's *d* effect sizes were extracted using multiple linear regressions, and pooled across research centres using random-effects meta-analysis. Cortical structures with *P*-values $< 1.49 \times 10^{-4}$ are shown in heatmap colours; strength of heat map is determined by the size of the Cohen's *d* ($d < 0$ = blue, $d > 0$ = yellow/red). Image generated using MATLAB with annotations added using Adobe Photoshop. An interactive version of this figure is available online, via 'ENIGMA-Viewer': http://enigma-viewer.org/ENIGMA_epilepsy_cortical.html. See Supplementary material for guidelines on how to use the interactive visualization. HS = hippocampal sclerosis.

and the left ($d = -0.42$; $P = 4.31 \times 10^{-6}$) and right precentral gyri ($d = -0.52$; $P = 1.25 \times 10^{-9}$). The MTLE-R subgroup also showed thickness changes in the left transverse temporal gyrus ($d = -0.31$; $P = 2.15 \times 10^{-5}$), and right pars opercularis ($d = -0.27$; $P = 1.45 \times 10^{-4}$) (Table 3 and Fig. 3C). By contrast, in MTLE-L, lower thickness was observed across six regions of the motor cortex, including the left ($d = -0.43$; $P = 1.61 \times 10^{-5}$) and right

paracentral gyri ($d = -0.38$; $P = 5.14 \times 10^{-7}$), left ($d = -0.47$; $P = 8.64 \times 10^{-9}$) and right precentral gyri ($d = -0.49$; $P = 2.37 \times 10^{-10}$), and left ($d = -0.54$; $P = 7.35 \times 10^{-5}$) and right precuneus ($d = -0.47$; $P = 5.16 \times 10^{-6}$). The MTLE-L group also showed thickness changes across five regions of the frontal cortex, including the left ($d = -0.41$; $P = 1.02 \times 10^{-11}$) and right superior frontal gyri ($d = -0.37$; $P = 1.44 \times 10^{-9}$), left ($d = -0.4$;

$P = 7.07 \times 10^{-9}$) and right caudal middle frontal gyri ($d = -0.44$; $P = 3.61 \times 10^{-7}$), and the right *pars triangularis* ($d = -0.29$; $P = 2.16 \times 10^{-6}$). In MTLE-L, thickness alterations were also observed in four regions of the temporal cortex, including the left temporopolar cortex ($d = -0.32$; $P = 3.33 \times 10^{-6}$), left parahippocampal gyrus ($d = -0.3$; $P = 3.95 \times 10^{-5}$), left entorhinal gyrus ($d = -0.45$; $P = 7.35 \times 10^{-10}$), and left fusiform gyrus ($d = -0.36$; $P = 2.19 \times 10^{-7}$) (Table 3 and Fig. 3B).

The IGE subgroup showed reduced thickness in the left ($d = -0.34$; $P = 1.75 \times 10^{-6}$) and right precentral gyri ($d = -0.39$; $P = 5.27 \times 10^{-8}$), when compared to healthy controls (Table 3 and Fig. 3D).

The all-other-epilepsies subgroup showed lower thickness across six cortical regions bilaterally, including the left ($d = -0.38$; $P = 1.76 \times 10^{-16}$) and right precentral gyri ($d = -0.35$; $P = 1.7 \times 10^{-14}$), left ($d = -0.26$; $P = 1.34 \times 10^{-8}$) and right paracentral gyri ($d = -0.35$; $P = 1.1 \times 10^{-14}$), left ($d = -0.29$; $P = 1.32 \times 10^{-10}$) and right caudal middle frontal gyri ($d = -0.21$; $P = 2.62 \times 10^{-6}$), left ($d = -0.22$; $P = 7.27 \times 10^{-7}$) and right superior parietal gyri ($d = -0.22$; $P = 1.15 \times 10^{-6}$), left ($d = -0.24$; $P = 3.51 \times 10^{-5}$) and right superior frontal gyri ($d = -0.23$; $P = 7.15 \times 10^{-6}$), and the left ($d = -0.18$; $P = 1.34 \times 10^{-4}$) and right precuneus ($d = -0.24$; $P = 7.78 \times 10^{-6}$) compared to controls. The all-other-epilepsies group also showed unilaterally reduced thickness in six right hemispheric regions, including the cuneus ($d = -0.23$; $P = 2.15 \times 10^{-7}$), lateral occipital gyrus ($d = -0.21$; $P = 3.18 \times 10^{-6}$), pars triangularis ($d = -0.21$; $P = 3.32 \times 10^{-6}$), supramarginal gyrus ($d = -0.21$; $P = 9.95 \times 10^{-6}$), transverse temporal gyrus ($d = -0.18$; $P = 6.84 \times 10^{-5}$), and lingual gyrus ($d = -0.18$; $P = 7.12 \times 10^{-5}$), compared to controls (Table 3 and Fig. 3E).

An interactive 3D visualization of these results is available via the ENIGMA-Viewer tool (Zhang *et al.*, 2017), at http://enigma-viewer.org/ENIGMA_epilepsy_cortical.html (Supplementary material). Cortical thickness differences significant after FDR adjustment can also be visualized at http://enigma-viewer.org/ENIGMA_epilepsy_cortical_fdr.html (Supplementary Tables 31–35).

Duration of illness, age at onset, and age-by-diagnosis effects on brain abnormalities

A secondary analysis identified significant associations between duration of epilepsy and several affected brain regions in the all-epilepsies, MTLE-R, and all-other-epilepsies groups. In the all-epilepsies group, duration of epilepsy negatively associated with volume measures in the left hippocampus ($b = -8.32$; $P = 8.16 \times 10^{-13}$), left ($b = -13.58$; $P = 3.52 \times 10^{-15}$), and right thalamus ($b = -12.25$; $P = 1.58 \times 10^{-13}$), and right pallidum ($b = -2.67$; $P = 1.78 \times 10^{-7}$), in addition to bilateral thickness measures in the left ($b = -0.003$; $P = 2.99 \times 10^{-11}$) and right pars

triangularis ($b = -0.002$; $P = 4.24 \times 10^{-9}$), left ($b = -0.003$; $P = 1.61 \times 10^{-15}$) and right caudal middle frontal gyri ($b = -0.003$; $P = 1.65 \times 10^{-17}$), left ($b = -0.003$; $P = 1.77 \times 10^{-13}$) and right supramarginal gyri ($b = -0.003$; $P = 2.58 \times 10^{-19}$), left ($b = -0.003$; $P = 5.84 \times 10^{-12}$) and right precentral gyri ($b = -0.003$; $P = 2.54 \times 10^{-24}$), left ($b = -0.004$; $P = 1.94 \times 10^{-12}$) and right superior frontal gyri ($b = -0.003$; $P = 4.65 \times 10^{-11}$), left ($b = -0.004$; $P = 1.05 \times 10^{-10}$) and right transverse temporal gyri ($b = -0.003$; $P = 8.24 \times 10^{-10}$), and left ($b = -0.002$; $P = 5.22 \times 10^{-6}$) and right paracentral gyri ($b = -0.002$; $P = 5.63 \times 10^{-6}$). Duration of epilepsy also negatively associated with unilateral thickness measures in the right precuneus ($b = -0.003$; $P = 6.03 \times 10^{-21}$), right pars opercularis ($b = -0.003$; $P = 5.59 \times 10^{-13}$), and right cuneus ($b = -0.002$; $P = 1.1 \times 10^{-9}$; Supplementary Table 8). In the MTLE-R subgroup, duration of epilepsy negatively associated with volume measures in the right hippocampus ($b = -22.42$; $P = 1.1 \times 10^{-7}$), and the right thalamus ($b = -18.11$; $P = 1.84 \times 10^{-5}$), and thickness measures in the left transverse temporal gyrus ($b = -0.007$; $P = 8.39 \times 10^{-5}$; Supplementary Table 8). In the all-other-epilepsies subgroup, duration of epilepsy negatively associated with bilateral thickness measures in the left ($b = -0.003$; $P = 3.39 \times 10^{-7}$) and right caudal middle frontal gyri ($b = -0.003$; $P = 6.91 \times 10^{-8}$), left ($b = -0.003$; $P = 1.36 \times 10^{-9}$) and right superior frontal gyri ($b = -0.003$; $P = 3.16 \times 10^{-7}$), and the left ($b = -0.003$; $P = 3.17 \times 10^{-5}$) and right precuneus ($b = -0.003$; $P = 5.01 \times 10^{-9}$), in addition to unilateral thickness measures in the right precentral gyrus ($b = -0.004$; $P = 1.16 \times 10^{-12}$), right cuneus ($b = -0.003$; $P = 8.57 \times 10^{-8}$), right pars triangularis ($b = -0.003$; $P = 5.16 \times 10^{-7}$), and right supramarginal gyrus ($b = -0.003$; $P = 2.24 \times 10^{-7}$). Duration of epilepsy also showed a positive association with the size of the left lateral ventricle in the all-other-epilepsies group ($b = 13.6$; $P = 1.17 \times 10^{-5}$).

In the all-epilepsies group, age at onset of epilepsy negatively associated with thickness measures in the left ($b = -0.003$; $P = 2.66 \times 10^{-15}$) and right superior frontal gyri ($b = -0.003$; $P = 9.77 \times 10^{-10}$), left ($b = -0.003$; $P = 2.78 \times 10^{-9}$) and right pars triangularis ($b = -0.003$; $P = 6.51 \times 10^{-7}$), right pars opercularis ($b = -0.003$; $P = 5.4 \times 10^{-14}$), left transverse temporal gyrus ($b = -0.003$; $P = 1.03 \times 10^{-8}$), and right cuneus ($b = -0.001$; $P = 4.9 \times 10^{-6}$). In the all-other-epilepsies subgroup, age at onset negatively correlated with thickness measures in the left ($b = -0.003$; $P = 3.21 \times 10^{-8}$) and right superior frontal gyri ($b = -0.002$; $P = 1.18 \times 10^{-4}$), left ($b = -0.002$; $P = 8.42 \times 10^{-6}$) and right precuneus ($b = -0.002$; $P = 7.23 \times 10^{-5}$), right pars triangularis ($b = -0.003$; $P = 2.53 \times 10^{-5}$), and right supramarginal gyrus ($b = -0.002$; $P = 2.38 \times 10^{-6}$). Age at onset also positively associated with the size of the right lateral ventricle in the all-other-epilepsies subgroup ($b = 57.73$; $P = 1.62 \times 10^{-7}$).

Age at onset negatively associated with other regional volumetric and thickness measures in the all-epilepsies, IGE, MTLE-L, MTLE-R, and all-other-epilepsies groups, but these associated areas showed no significant structural differences in the primary case-control analysis (Table 1 and Supplementary Table 8).

There were no interaction effects between age and syndromic diagnosis in the all-epilepsies, MTLE-L, MTLE-R, IGE, or all-other-epilepsies groups.

Power analyses for detection of case-control differences

In our sample of 2149 individuals with epilepsy and 1727 healthy controls, we had 80% power to detect Cohen's d effect sizes as small as $d = 0.091$ at the standard alpha level of $P < 0.05$ (two-tailed), and 80% power to detect Cohen's d effect sizes as small as $d = 0.149$ at the study's stringent Bonferroni-corrected threshold of $P < 1.49 \times 10^{-4}$.

N_{80}, the number of cases and controls required to achieve 80% power to detect group differences using a two-tailed t-test at $P < 0.05$, ranged from $N_{80} = 6$, to detect group effects in the right hippocampus in our MTLE-R group, to $N_{80} = 503$, to detect group effects in the right pars opercularis in our 'all epilepsies' group (Tables 2 and 3).

Discussion

In the largest coordinated neuroimaging study of epilepsy to date, we identified a series of quantitative imaging signatures—some shared across common epilepsy syndromes, and others characteristic of selected, specific epilepsy syndromes. Our sample of 2149 individuals with epilepsy and 1727 controls provided 80% power to detect differences as small as $d = 0.091$ ($P < 0.05$, two-tailed), allowing us to identify subtle, consistent brain abnormalities that are typically undetectable on visual inspection, or overlooked using smaller case-control designs. This international collaboration addresses prior inconsistencies in the field of epilepsy neuroimaging, providing a robust, *in vivo* map of structural aberrations, upon which future studies of disease mechanisms may expand.

In the first of five cross-sectional MRI analyses, we investigated a diverse aggregation of epilepsy syndromes, putative causes, and durations of disease. This all-epilepsies group exhibited shared, diffuse brain structural differences across several regions including the thalamus, pallidum, precentral, paracentral, and superior frontal cortices. With the exception of hippocampal volume and entorhinal thickness differences (Supplementary material), these structural alterations were not driven by any specific syndrome or dataset (Supplementary Figs 3 and 7). Our findings suggest a common neuroanatomical signature of epilepsy across a wide spectrum of disease types, complementing recent evidence for shared genetic susceptibility to a wide spectrum

of epilepsies (International League Against Epilepsy Consortium on Complex Epilepsies, 2014). Some structural and genetic pathways may be shared across syndromes, despite the heterogeneity of epilepsy and seizure types. This shared MRI signature underpins the contemporary shift towards the study of epilepsies as network phenomena (Caciagli *et al.*, 2014).

In MTLE, as expected, we observed hippocampal volume abnormalities ipsilateral to the patient's side of seizure onset. Neither MTLE-L nor MTLE-R showed significant contralateral hippocampal volume reductions, confirming that sporadic, unilateral MTLE is not routinely underpinned by bilateral hippocampal damage (Blümcke *et al.*, 2013). Both MTLE groups showed extrahippocampal abnormalities in the ipsilateral thalamus and pallidum, with widespread reductions in cortical thickness, supporting a growing body of literature indicating that MTLE, as an example of a specific disease constellation in the epilepsies, is also a network disease, extending beyond the mesial temporal regions (Keller *et al.*, 2014; de Campos *et al.*, 2016). Disruption of this network, notably in the thalamus (Keller *et al.*, 2015; He *et al.*, 2017) and thalamo-temporal white matter tracts (Keller *et al.*, 2015, 2017), may be associated with postoperative seizure outcome in MTLE.

Patients with left and right MTLE showed distinct patterns of structural abnormalities when compared to controls, resolving conflicting findings from smaller studies, some reporting an equal distribution of structural differences (Liu *et al.*, 2016), and others indicating more diffuse abnormalities, either in left MTLE (Keller *et al.*, 2002, 2012; Bonilha *et al.*, 2007; Kemmotsu *et al.*, 2011; de Campos *et al.*, 2016) or in right MTLE (Pail *et al.*, 2009). The structural differences observed in the present study may reflect a younger age at onset of epilepsy in left MTLE, which occurred, on average, 1.2 years earlier than those with right MTLE (Supplementary Table 20). Independent, large-scale studies of MTLE patients have confirmed a significantly earlier age at onset in left, compared to right, MTLE (Blümcke *et al.*, 2017). Duration-related effects were also observed in right, but not left, MTLE, pointing to possible biological distinctions between the two.

In IGE, a clinically and biologically distinct group of epilepsies typically associated with 'normal' MRI on clinical inspection (Woermann *et al.*, 1998), we identified reduced volume of the right thalamus, and thinner precentral gyri in both hemispheres, supporting prior reports of structural (Bernhardt *et al.*, 2009*a*), electroencephalographic, and functional (Gotman *et al.*, 2005) abnormalities in IGE. These IGE cases were considered typical by reviewing neurologists, suggesting that this common type of epilepsy is also associated with quantifiable structural brain abnormalities.

The precentral gyri, site of the primary motor cortex, showed bilateral structural deficits across all epilepsy groups (all-epilepsies, IGE, MTLE-L, MTLE-R, and all-other-epilepsies), without detectable inter-cohort or between-disease heterogeneity (Supplementary Figs 3–12).

Atrophy of the motor cortex has been linked to seizure frequency and duration of epilepsy in MTLE (Coan *et al.*, 2014); here, we observed a negative correlation between precentral (and postcentral) grey matter thickness and duration of epilepsy in the aggregate all-epilepsies group.

The right thalamus also showed evidence of structural compromise across all epilepsy cohorts, re-emphasizing the importance of the thalamus as a major hub in the epilepsy network (He *et al.*, 2017; Jobst and Cascino, 2017). Loss of feed-forward inhibition between the thalamus and its neocortical connections may be epileptogenic (Paz and Huguenard, 2015), and thalamocortical abnormalities have previously been reported in IGE (Gotman *et al.*, 2005; Bernhardt *et al.*, 2009a; O'Muircheartaigh *et al.*, 2012) and MTLE (Mueller *et al.*, 2010; Bernhardt *et al.*, 2012). These findings support prior 'system epilepsies' hypotheses of pathophysiology (Avanzini *et al.*, 2012), suggesting that a broad range of common epilepsies share vulnerability within a thalamocortical structural pathway involved in, and likely affected by, seizures (Liu *et al.*, 2003; Bernhardt *et al.*, 2013). Given this study's cross-sectional design, we cannot determine if these are causative changes, consequences of recurrent seizures, prolonged drug treatment, or a combination of factors. The epilepsies, as a broad group, may involve progressive structural change (Caciagli *et al.*, 2017), indicating the need for large-scale longitudinal studies.

A heterogeneous subgroup of individuals without confirmed diagnoses of IGE or MTLE with hippocampal sclerosis showed similar patterns of structural alterations to those observed in the aggregate all-epilepsies cohort. The findings included enlarged ventricles, smaller right pallidum and right thalamus, and reduced thickness across the motor and frontal cortices. Hippocampal abnormalities were not observed in this subgroup, suggesting that the patterns of reduced hippocampal grey matter observed in the aggregate group were driven by the inclusion of MTLEs with hippocampal sclerosis. Unlike the IGE, MTLE, and aggregate epilepsy cohorts, this subgroup also showed bilateral enlargement of the amygdala—a phenomenon previously reported in non-lesional localization-related epilepsies (Reyes *et al.*, 2017) and non-lesional MTLEs (Takaya *et al.*, 2012; Coan *et al.*, 2013). Non-lesional MTLEs formed a large proportion of this 'all-other-epilepsies' cohort (43.3%; 445 individuals), but the subgroup included many other focal and unclassified syndromes, potentially obscuring specific biological interpretations. Future, sufficiently powered studies will stratify this cohort into finer-grained subtypes to delineate syndrome-specific effects.

Despite its international scale, our study has limitations. All results were derived from cross-sectional data: we cannot distinguish between historical acute damage and progressive abnormalities. We cannot disentangle the relative contributions of environmental and treatment-related factors, including antiepileptic medications, seizure types and frequencies, disease severity, language dominance, and other initial precipitating factors. On average, duration of epilepsy was at least 10 years; longitudinal investigations of new-onset and paediatric epilepsies will provide a more comprehensive understanding. Despite using standardized image processing protocols, quality control, and statistical techniques, some brain measures showed a wide distribution of effect sizes across research centres, which may reflect sample heterogeneity and differences in scanning protocols (Supplementary material).

We observed modest thickness differences across the majority of cortical regions; Cohen's *d* effect sizes ranged from small to moderate ($d = 0.2$–0.5), with some very small effects ($d < 0.2$) noted in the right pars opercularis, bilateral pars triangularis, and bilateral transverse temporal gyri of the aggregate all-epilepsies group. Other large-scale ENIGMA studies have reported similarly modest (albeit less widespread) cortical abnormalities in psychiatric illnesses including major depression (Schmaal *et al.*, 2016) and bipolar disorder (Hibar *et al.*, 2017b). Although epilepsy is characterized by an enduring predisposition to generate abnormal excessive or synchronous neuronal activity in the brain (Fisher *et al.*, 2014), our findings indicate that common epilepsies are associated with widespread, but relatively subtle, structural alterations of the neocortex. Replication in independent MRI cohorts, complemented by advanced imaging modalities and large-scale gene expression datasets, will help elucidate how these cortical abnormalities relate to underlying disease processes.

Overall, in the largest neuroimaging analysis of epilepsy to date, we demonstrate a pattern of robust brain structural abnormalities within and between syndromes. Specific functional interpretations cannot be inferred from grey matter differences, but lower volume and thickness measures may reflect tissue loss, supporting recent observations that the common epilepsies cannot always be considered benign (Gaitatzis *et al.*, 2004; Bell *et al.*, 2016; Devinsky *et al.*, 2017). The study provides a macroscopic neuroanatomical map upon which neuropathological work, animal models, and further gene expression studies, can expand. Our consortium plans to investigate more specific neuroanatomical traits and epilepsy phenotypes, explore sophisticated shape and sulcal measures, and eventually conduct genome-wide association analysis of brain measures, to improve our understanding and treatment of the epilepsies.

Web resources

All image processing, quality assurance, and statistical analysis protocols for this study can be downloaded from the ENIGMA website, at: http://enigma.usc.edu/ongoing/enigma-epilepsy/enigma-epilepsy-protocols/.

Acknowledgements

Funding

Supplementary material

Supplementary material is available at *Brain* online.

References

Adams HH, Hibar DP, Chouraki V, Stein JL, Nyquist PA, Rentería ME, et al. Novel genetic loci underlying human intracranial volume identified through genome-wide association. Nat Neurosci 2016; 19: 1569–82.

Alvim MK, Coan AC, Campos BM, Yasuda CL, Oliveira MC, Morita ME, Cendes F. Progression of gray matter atrophy in seizure-free patients with temporal lobe epilepsy. Epilepsia 2016; 57; 621–9.

Avanzini G, Manganotti P, Meletti S, Moshé SL, Panzica F, Wolf P, et al. The system epilepsies: a pathophysiological hypothesis. Epilepsia 2012; 53: 771–8.

Bearden CE, Thompson PM. Emerging global initiatives in neurogenetics: the Enhancing Neuroimaging Genetics Through Meta-Analysis (ENIGMA) Consortium. Neuron 2017; 94: 232–6.

Bell GS, Neligan A, Giavasi C, Keezer MR, Novy J, Peacock JL, et al. Outcome of seizures in the general population after 25 years: a prospective follow-up, observational cohort study. J Neurol Neurosurg Psychiatry 2016; 87: 843–50.

Bell GS, Neligan A, Sander JW. An unknown quantity—the worldwide prevalence of epilepsy. Epilepsia 2014; 55: 958–62.

Benjamini Y, Hochberg Y. Controlling the false discovery rate: a practical and powerful approach to multiple testing. J R Stat Soc 1995; 57: 289–300.

Ben-Menachem E. Epilepsy in 2015: the year of collaborations for big data. Lancet Neurol 2016; 15: 6–7.

Berg AT, Berkovic SF, Brodie MJ, Buchhalter J, Cross JH, van Emde Boas W, et al. Revised terminology and concepts for organization of seizures and epilepsies: report of the ILAE Commission on Classification and Terminology, 2005-2009. Epilepsia 2010; 51: 676–85.

Bernasconi N. Is epilepsy a curable neurodegenerative disease? Brain 2016; 139: 2336–7.

Bernhardt BC, Bernasconi N, Concha L, Bernasconi A. Cortical thickness analysis in temporal lobe epilepsy: reproducibility and relation to outcome. Neurology 2010; 74: 1776–84.

Bernhardt BC, Bernasconi N, Kim H, Bernasconi A. Mapping thalamocortical network pathology in temporal lobe epilepsy. Neurology 2012; 78: 129–36.

Bernhardt BC, Bonilha L, Gross DW. Network analysis for a network disorder: the emerging role of graph theory in the study of epilepsy. Epilepsy Behav 2015; 50: 162–70.

Bernhardt BC, Kim H, Bernasconi N. Patterns of subregional mesiotemporal disease progression in temporal lobe epilepsy. Neurology 2013; 81: 1840–7.

Bernhardt BC, Rozen DA, Worsley KJ, Evans AC, Bernasconi N, Bernasconi A. Thalamo–cortical network pathology in idiopathic generalized epilepsy: insights from MRI-based morphometric correlation analysis. Neuroimage 2009a; 46: 373–81.

Bernhardt BC, Worsley KJ, Kim H, Evans AC, Bernasconi A, Bernasconi N. Longitudinal and cross-sectional analysis of atrophy in pharmacoresistant temporal lobe epilepsy. Neurology 2009b; 72: 1747–54.

Betting LE, Mory SB, Lopes-Cendes I, Li LM, Guerreiro MM, Guerreiro CAM, et al. MRI reveals structural abnormalities in patients with idiopathic generalized epilepsy. Neurology 2006; 67: 848–52.

Blanc F, Martinian L, Liagkouras I, Catarino C, Sisodiya SM, Thom M. Investigation of widespread neocortical pathology associated with hippocampal sclerosis in epilepsy: a postmortem study. Epilepsia 2011; 52: 10–21.

Blümcke I, Spreafico R, Haaker G, Coras R, Kobow K, Bien CG, Pfäfflin M, et al. Histopathological findings in tissue obtained from epilepsy surgery. N Engl J Med 2017; 377: 1648–56.

Blümcke I, Thom M, Aronica E, Armstrong DD, Bartolomei F, Bernasconi A, et al. International consensus classification of hippocampal sclerosis in temporal lobe epilepsy: a task force report from the ILAE Commission on Diagnostic Methods. Epilepsia 2013; 54: 1315–29.

Boedhoe PSW, Abe Y, Ameis SH, Arnold PD, Batistuzzo MC, Benedetti F, et al. Distinct subcortical volume alterations in pediatric and adult OCD: a worldwide meta- and mega-analysis. AJP 2017; 174: 60–9.

Bonilha L, Rorden C, Halford JJ, Eckert M, Appenzeller S., et al. Asymmetrical extra-hippocampal grey matter loss related to hippocampal atrophy in patients with medial temporal lobe epilepsy. J Neurol Neurosurg Psychiatry 2007; 78: 286–94.

Button KS, Ioannidis JPA, Mokrysz C, Nosek BA, Flint J, Robinson ESJ, et al. Power failure: why small sample size undermines the reliability of neuroscience. Nat Rev Neurosci 2013; 14: 365–76.

Caciagli L, Bernhardt BC, Hong S-J, Bernasconi A, Bernasconi N. Functional network alterations and their structural substrate in drug-resistant epilepsy. Front Neurosci 2014; 8: 411.

Caciagli L, Bernasconi A, Wiebe S, Koepp MJ, Bernasconi N, Bernhardt BC. A meta-analysis on progressive atrophy in intractable temporal lobe epilepsy: time is brain? Neurology 2017; 89: 506–16.

Coan AC, Campos BM, Yasuda CL, Kubota BY, Bergo FP, Guerreiro CA, et al. Frequent seizures are associated with a network of gray matter atrophy in temporal lobe epilepsy with or without hippocampal sclerosis. PLoS One 2014; 9: e85843.

Coan AC, Morita ME, de Campos BM, Yasuda C, Cendes F. Amygdala enlargement in patients with mesial temporal lobe epilepsy without hippocampal sclerosis. Front Neurol 2013; 4: 1–5.

de Campos B, Coan A, Yasuda C, Casseb R, Cendes F. Large-scale brain networks are distinctly affected in right and left mesial temporal lobe epilepsy. Hum Brain Mapp 2016; 37: 3137–52.

Devinsky O, Friedman D, Cheng JY, Moffatt E, Kim A, Tseng ZH. Underestimation of sudden deaths among patients with seizures and epilepsy. Neurology 2017; 89: 886–92.

Englot DJ, Chang EF, Auguste KI. Vagus nerve stimulation for epilepsy: a meta-analysis of efficacy and predictors of response. J Neurosurg 2011; 115: 1248–55.

Fischl B. FreeSurfer. Neuroimage 2012; 62: 774–81.

Fisher RS, Acevedo C, Arzimanoglou A, Bogacz A, Cross JH, et al. ILAE official report: a practical clinical definition of epilepsy. Epilepsia 2014; 55: 475–82.

French JA. Refractory epilepsy: clinical overview. Epilepsia 2007; 48: 3–7.

Gaitatzis A, Johnson AL, Chadwick DW, Shorvon SD, Sander JW. Life expectancy in people with newly diagnosed epilepsy. Brain 2004; 127: 2427–32.

Gotman J, Grova C, Bagshaw A, Kobayashi E, Aghakhani Y, Dubeau F. Generalized epileptic discharges show thalamocortical activation and suspension of the default state of the brain. Proc Natl Acad Sci USA 2005; 102: 15236–240.

Hansen TI, Brezova V, Eikenes L, Haberg A, Vangberg TR. How does the accuracy of intracranial volume measurements affect normalized brain volumes? Sample size estimates based on 966 subjects from the HUNT MRI cohort. AJNR Am J Neuroradiol 2015; 36: 1450–6.

He X, Doucet GE, Pustina D, Sperling MR, Sharan AD, Tracy JI. Presurgical thalamic "hubness" predicts surgical outcome in temporal lobe epilepsy. Neurology 2017; 88: 2285–93.

Hibar DP, Adams HHH, Jahanshad N, Chauhan G, Stein JL, Hofer E, et al. Novel genetic loci associated with hippocampal volume. Nat Commun 2017a; 8: 13624.

Hibar DP, Stein JL, Rentería ME, Arias-Vasquez A, Desrivières S, Jahanshad N, et al. Common genetic variants influence human subcortical brain structures. Nature 2015; 520: 224–9.

Hibar DP, Westlye LT, Doan NT, Jahanshad N, Cheung JW, Ching CRK, et al. Cortical abnormalities in bipolar disorder: an MRI analysis of 6503 individuals from the ENIGMA bipolar disorder working group. Mol Psychiatry 2017b, in press.

Hibar DP, Westlye LT, van Erp TGM, Rasmussen J, Leonardo CD, Faskowitz J, et al. Subcortical volumetric abnormalities in bipolar disorder. Mol Psychiatry 2016; 21: 1710–16.

Hoogman M, Bralten J, Hibar DP, Mennes M, Zwiers MP, Schweren LSJ, et al. Subcortical brain volume differences in participants with attention deficit hyperactivity disorder in children and adults: a cross-sectional mega-analysis. Lancet Psychiatry 2017; 4: 310–19.

International League Against Epilepsy Consortium on Complex Epilepsies. Genetic determinants of common epilepsies: a meta-analysis of genome-wide association studies. Lancet Neurol 2014; 13: 893–903.

Jobst BC and Cascino GD. Thalamus as a "hub" to predict outcome after epilepsy surgery. Neurology 2017; 88: 2246–7.

Keller SS, Glenn GR, Weber B, Kreilkamp BAK, Jensen JH, et al. Preoperative automated fibre quantification predicts postoperative seizure outcome in temporal lobe epilepsy. Brain 2017; 140: 68–2.

Keller SS, Mackay CE, Barrick TR, Wieschmann UC, Howard MA, Roberts N. Voxel-based morphometric comparison of hippocampal and extrahippocampal abnormalities in patients with left and right hippocampal atrophy. Neuroimage 2002; 16: 23–31.

Keller SS, O'Muircheartaigh J, Traynor C, Towgood K, Barker G, Richardson MP. Thalamotemporal impairment in temporal lobe epilepsy: a combined MRI analysis of structure, integrity, and connectivity. Epilepsia 2014; 55: 306–15.

Keller SS, Richardson MP, Schoene-Bake J, O'Muircheartaigh J, et al. Thalamotemporal alteration and postoperative seizures in temporal lobe epilepsy. Ann Neurol 2015; 77: 760–74.

Keller SS, Roberts N. Voxel-based morphometry of temporal lobe epilepsy: an introduction and review of the literature. Epilepsia 2008; 49; 741–57.

Keller SS, Schoene-Bake S, Gerdes JS, Weber B, Deppe M. Concomitant fractional anisotropy and volumetric abnormalities in temporal lobe epilepsy: cross-sectional evidence for progressive neurologic injury. PLoS One 2012; 7; e46791.

Kemmotsu N, Girard HM, Bernhardt BC, Bonilha B, Lin JJ, Tecoma ES, et al. MRI analysis in temporal lobe epilepsy: cortical thinning and white matter disruptions are related to side of seizure onset. Epilepsia 2011; 52: 2257–66.

Labate A, Cerasa A, Aguglia U, Mumoli L, Quattrone A, Gambardella A. Neocortical thinning in 'benign' mesial temporal lobe epilepsy. Epilepsia 2011; 52: 712–17.

Liu M, Bernhardt BC, Bernasconi A, Bernasconi N. Gray matter structural compromise is equally distributed in left and right temporal lobe epilepsy. Human Brain Mapping 2016; 37: 515–24.

Liu RSN, Lemieux L, Bell GS, Hammers A, Sisodiya SM, Bartlett PA, et al. Progressive neocortical damage in epilepsy. Ann Neurol 2003; 53: 312–24.

Mueller SG, Laxer KD, Barakos J, Cheong I, Finlay D, Garcia P, et al. Involvement of the thalamocortical network in TLE with and without mesiotemporal sclerosis. Epilepsia 2010; 51: 1436–45.

Nickels KC, Zaccariello MJ, Hamiwka LD, Wirrell EC. Cognitive and neurodevelopmental comorbidities in paediatric epilepsy. Nat Rev Neurol 2016; 12: 465–76.

O'Muircheartaigh J, Vollmar C, Barker GJ, Kumari V, Symms MR, et al. Focal structural changes and cognitive dysfunction in juvenile myoclonic epilepsy. Neurology 2011; 76: 34–40.

O'Muircheartaigh J, Vollmar C, Barker GJ, Kumari V, Symms MR, et al. Abnormal thalamocortical structural and functional connectivity in juvenile myoclonic epilepsy. Brain 2012; 135: 3635–44.

Overvliet GM, Besseling RMH, Jansen JFA, van der Kruijs SJM, Vles JSH, Hofman PAM, et al. Early onset of cortical thinning in children with rolandic epilepsy. Neuroimage Clin 2013; 2: 434–9.

Pail M, Brázdil M, Mareček R, Mikl M. An optimized voxel-based morphometric study of gray matter changes in patients with left-sided and right-sided mesial temporal lobe epilepsy and hippocampal sclerosis (MTLE/HS). Epilepsia 2009; 51: 511–18.

Paz JT, Huguenard JR. Microcircuits and their interactions in epilepsy: is the focus out of focus? Nat Neurosci 2015; 18: 351–9.

Pitkänen A, Löscher W, Vezzani A, Becker AJ, Simonato M, Lukasiuk K, et al. Advances in the development of biomarkers for epilepsy. Lancet Neurol 2016; 15: 843–56.

Reyes A, Thesen T, Kuzniecky R, Devinsky O, McDonald CR, et al. Amygdala enlargement: temporal lobe epilepsy subtype or nonspecific finding? Epilepsy Res 2017; 132: 34–40.

Ronan L, Alhusaini S, Scanlon C, Doherty CP, Delanty N, Fitzsimons M. Widespread cortical morphologic changes in juvenile myoclonic epilepsy: evidence from structural MRI. Epilepsia 2012; 53: 651–8.

Scheffer IE, Berkovic S, Capovilla G, Connolly MB, French J, et al. ILAE Classification of the epilepsies: position paper of the ILAE Commission for Classification and Terminology. Epilepsia 2017; 58: 512–21.

Schmaal L, Hibar DP, Sämann PG, Hall GB, Baune BT, Jahanshad N, et al. Cortical abnormalities in adults and adolescents with major depression based on brain scans from 20 cohorts worldwide in the ENIGMA Major Depressive Disorder Working Group. Mol Psychiatry 2016; 22: 900–9.

Schmaal L, Veltman DJ, van Erp TGM, Sämann PG, Frodl T, Jahanshad N, et al. Subcortical brain alterations in major depressive disorder: findings from the ENIGMA Major Depressive Disorder working group. Mol Psychiatry 2015; 21: 806–12.

Stein JL, Medland SE, Vasquez AA, Hibar DP, Senstad RE, Winkler AM, et al. Identification of common variants associated with human hippocampal and intracranial volumes. Nat Genet 2012; 44: 552–61.

Takaya S, Ikeda A, Takahiro M-O, Matsumoto R, Inouchi M, et al. Temporal lobe epilepsy with amygdala enlargement: a morphological and functional study. J Neuroimaging 2012; 24: 54–62.

Téllez-Zenteno JF, Dhar R, Wiebe S. Long-term seizure outcomes following epilepsy surgery: a systematic review and meta-analysis. Brain 2005; 128: 1188–98.

Thom M, Eriksson S, Martinian L, Caboclo LO, McEvoy AW, Duncan JS, et al. Temporal lobe sclerosis associated with hippocampal sclerosis in temporal lobe epilepsy: neuropathological features. J Neuropathol Exp Neurol 2009; 68: 928–38.

Thompson PM, Andreassen OA, Arias-Vasquez A, Bearden CE, Boedhoe PS, Brouwer RM, et al. ENIGMA and the individual: predicting factors that affect the brain in 35 countries worldwide. Neuroimage 2017; 145: 389–408.

Vaughan D, Rayner G, Tailby C, Jackson GD. MRI-negative temporal lobe epilepsy: a network disorder of neocortical connectivity. Neurology 2016; 87: 1934–42.

van Erp TGM, Hibar DP, Rasmussen JM, Glahn DC, Pearlson GD, Andreassen OA, et al. Subcortical brain volume abnormalities in 2028 individuals with schizophrenia and 2540 healthy controls via the ENIGMA consortium. Mol Psychiatry 2016; 21: 547–53.

Viechtbauer W. Conducting meta-analyses in R with the metafor package. J Stat Soft 2010; 36.

Vlooswijk MC, Jansen JF, de Krom MC, Majoie HM, Hofman PA, Backes WH, et al. Functional MRI in chronic epilepsy: associations with cognitive impairment. Lancet Neurol 2010; 9: 1018–27.

Vollmar CV, O'Muircheartaigh J, Barker GJ, Symms MR, Thompson P, et al. Motor system hyperconnectivity in juvenile myoclonic epilepsy: a cognitive functional magnetic resonance imaging study. Brain 2011; 134: 1710–19.

Woermann FG, Sisodiya SM, Free SL, Duncan JS. Quantitative MRI in patients with idiopathic generalized epilepsy. Evidence of widespread cerebral structural changes. Brain 1998; 121: 1661–7.

Zhang G, Kochunov P, Hong E, Kelly S, Whelan CD, Jahanshad N, et al. ENIGMA-viewer: interactive visualization strategies for conveying effect sizes in meta-analysis. BMC Bioinformatics 2017; 18 (Suppl 6): 253.